frontiers | Frontiers in Astronomy and Space Sciences

ORIGINAL RESEARCH
published: 04 April 2022
doi: 10.3389/fspas.2022.858300

Magnetic Fluctuations Associated With Small-Scale Magnetic Holes in the Martian Magnetosheath

Yangjun Chen[1,2], Mingyu Wu[1], Sudong Xiao[1], Aimin Du[3], Guoqiang Wang[1], Yuanqiang Chen[1], Zonghao Pan[2] and Tielong Zhang[1,2,4]**

[1]Institute of Space Science and Applied Technology, Harbin Institute of Technology, Shenzhen, China, [2]Key Laboratory of Geospace Environment, Chinese Academy of Sciences, University of Science and Technology of China, Hefei, China, [3]Institute of Geology and Geophysics, Chinese Academy of Sciences, Beijing, China, [4]Space Research Institute, Austrian Academy of Sciences, Graz, Austria

OPEN ACCESS

Edited by:
Olga V. Khabarova, Institute of Terrestrial Magnetism ionosphere and Radio Wave Propagation (RAS), Russia

Reviewed by:
Ezequiel Echer, National Institute of Space Research (INPE), Brazil
Wenya Li, National Space Science Center (CAS), China

***Correspondence:**
Mingyu Wu
wumingyu@hit.edu.cn
Tielong Zhang
tielong.zhang@oeaw.ac.at

Specialty section:
This article was submitted to Space Physics, a section of the journal Frontiers in Astronomy and Space Sciences

Received: *19 January 2022*
Accepted: *07 March 2022*
Published: *04 April 2022*

Citation:
Chen Y, Wu M, Xiao S, Du A, Wang G, Chen Y, Pan Z and Zhang T (2022) Magnetic Fluctuations Associated With Small-Scale Magnetic Holes in the Martian Magnetosheath. Front. Astron. Space Sci. 9:858300. doi: 10.3389/fspas.2022.858300

Small-scale magnetic holes are common magnetic structures with a spatial scale always smaller than one thermal proton gyroradius (ρ_i) in the turbulent planetary magnetosheath. However, the contribution of small-scale MHs to dissipating energy and transporting particles in turbulent plasmas is still unclear. In this work, we investigate magnetic fluctuations around small-scale MHs in the Martian magnetosheath and compute their spectral indices in the kinetic frequency range. Our statistical results show that the spectral index value gradually decreases from the bow shock to the induced magnetosphere boundary at the nightside of Mars. Small-scale MHs have an obvious influence on the spectral indices of the magnetic fluctuations by their high-frequency components. For most events, these MHs lead to a variation in the spectral index in the kinetic range, and such a variation can be very significant in more than 20% of events. Our results indicate that because of the existence of MHs, using the spectral index alone as a diagnostic sometimes is not enough convincing during the analysis of turbulence in planetary environments.

Keywords: small-scale magnetic holes, Mars, magnetic fluctuations, spectral indices, magnetosheath

INTRODUCTION

Unlike Earth, Mars is an unmagnetized planet without a global intrinsic magnetic field (Acuña et al., 1998). Therefore, the shock supermagnetosonic solar wind can directly interact with the Martian ionosphere and then both a bow shock and an induced magnetosphere boundary are formed as two important boundaries which can divide the Martian space environment into three parts: the upstream solar wind, the magnetosheath, and the induced magnetosphere (Zhang et al., 1991; Bertucci et al., 2004). The Martian magnetosheath is full of magnetized plasma and strong magnetic fluctuations (Ruhunusiri et al., 2017). Magnetic fluctuations and turbulence can play a key role in the particle acceleration and heating of space plasma (Zimbardo et al., 2010; Bruno and Carbone, 2013), which can deeply affect the interaction between the solar wind and Mars.

The spectral indices are widely used to analyze the properties of magnetic fluctuations and turbulence in the various space plasma environments, such as the solar wind (Alexandrova et al., 2008; Kiyani et al., 2009) and the magnetosphere of Mercury (Uritsky et al., 2011), Venus (Vörös et al., 2008; Xiao et al., 2018), Earth (Vörös et al., 2004; Sahraoui et al., 2006), and Mars (Ruhunusiri et al., 2017). These fluctuations have power–law relationships as $P \propto f^{-\alpha}$, where P is power spectral density, f is frequency, and α is the spectral index. The spectral index provides the physical information in a certain frequency range, such as energy injection, cascade, and dissipation (e.g., Bowen et al., 2021). The values of the spectral index are different in the magnetohydrodynamic (MHD) frequency range and kinetic range. In the MHD range, the spectral index of turbulence has the Kolmogorov scaling value of α ~ 5/3 classical Kolmogorov spectrum (Goldstein et al., 1995; Alexandrova, 2008; Bruno and Carbone, 2013). Energy cascades are considered to occur in this range, where energy is transported from a lower frequency to a higher frequency. The magnetic energy dissipates into plasma in the kinetic range, where the turbulence spectral index is near 2.8 (e.g., Roberts et al., 2015). Ruhunusiri et al. (2017) have found that the spectral index value is mainly between 2.4 and 2.9 for the kinetic range in the Martian magnetosheath. The features of magnetic turbulence can be affected by the geometry of the bow shock, plasma beta, and some instabilities (e.g., Hollweg and Markovskii, 2002; Chen et al., 2009; Xiao et al., 2018; Vörös et al., 2019; Bowen et al., 2021; Xiao et al., 2021). However, differences in the kinetic range turbulence resulting from the sub-proton scale coherent structures in the Martian magnetosheath are still an open question.

Recently, a sub-proton scale coherent magnetic structure, called small-scale magnetic holes (MHs), has been widely reported in the solar wind and plasma sheet (Ge et al., 2011; Sun et al., 2012; Sundberg et al., 2015; Gershman et al., 2016; Wang et al., 2020a). Meanwhile, these structures are reported in highly turbulent environments like the terrestrial magnetosheath (Huang et al., 2017a; Huang et al., 2017b; Yao et al., 2017; Yao et al., 2020), Venusian magnetosheath (Goodrich et al., 2021), and Martian magnetosheath (Wu et al., 2021). The small-scale MH manifests itself as a depletion in magnetic field strength with a spatial scale less than one thermal proton gyroradius (ρ_i) or on the order of ρ_i. The observational features of small-scale MHs suggest that such a structure could be an electron current loop or an electron-scale vortex (Wang et al., 2020b). The large-scale magnetic holes with a spatial scale from tens to hundreds of ρ_i are suggested to be formed by the proton mirror mode (Tsurutani et al., 2010; Tsurutani et al., 2011). However, due to the size of small-scale MHs, such MHD range cannot be worked during their formation. Now, the generation mechanism of small-scale MHs is an open question. Although there are several suggested mechanisms like the electron mirror instability (Ge et al., 2011) and the tearing instability (Balikhin et al., 2012), they have not been observationally confirmed until now. Additionally, the particle-in-cell (PIC) simulations performed by Haynes et al. (2015) and Roytershteyn et al. (2015) have suggested that small-scale MHs can arise as a coherent structure in turbulence. The differences in the turbulence caused by wave activity like small-scale magnetic holes in the Martian magnetosheath are not still clear.

Based on the measurements from the Mars Atmosphere and Volatile Evolution (MAVEN) mission, we investigate the kinetic scale magnetic fluctuations in the Martian magnetosheath and focus on the events containing the small-scale magnetic holes. We analyze the effect of the small-scale magnetic holes on the kinetic scale magnetic fluctuations in this study.

Data Set and Methods

MAVEN (Jakosky et al., 2015) was launched in November 2013 and was designed to explore the Martian upper atmosphere, ionosphere, and interactions between Mars and the solar wind. MAVEN has a tilted elliptical orbit with a perigee of 150 km and an apogee of 6,220 km. The orbital period of MAVEN around Mars is about 4.5 h. MAVEN spends much time in the Martian magnetosheath and collects a vast amount of data to study small-scale MHs in the Martian magnetosheath. In this study, we use 32-Hz magnetic field data from the magnetometer (Connerney et al., 2015). The Mars Solar Orbital (MSO) coordinate system is used unless otherwise specified. The MSO is a right-handed system whose X axis points toward the Sun from Mars, Z axis is perpendicular to the Martian ecliptic plane and points toward the north pole of Mars, and Y axis completes the coordinate system.

We identified small-scale MHs by a similar criterion used in Wu et al. (2021). The magnetic field amplitude depression B_{min}/B is smaller than 0.75, and the boundaries of the MHs are defined by a magnitude larger than B – δ, where B_{min}, B, and δ are the minimum, the average, and the deviation of the magnetic field magnitude within 5-s windows surrounding the center of the hole, respectively. The rotation angle $\Delta\varphi$ is calculated by the magnetic field vectors at the two boundaries of the MHs. We select MH events with the rotation angles smaller than 15°. If the time interval between two small-scale MHs is shorter 2 s, they are merged into one event. Similar criteria are also used in the selection of MHs in the Venusian space environment and terrestrial magnetosheath (Zhang et al., 2008; Zhang et al., 2009). Due to the high occurrence rate of small-scale MHs in the magnetosheath, even in 1 month, there are plenty of events (Wu et al., 2021). Therefore, we used February 2016 events and totally found 137 small-scale magnetic hole events from this month by our selection criteria. The size of these MHs in this month has already been analyzed before (Wu et al., 2021). As shown in **Figure 5** of Wu et al. (2021), the spatial scale of all 137 events used in this article is less than or on the order of the proton gyroradius.

For the analysis of the magnetic fluctuation and turbulence associated with small-scale MHs in the Martian magnetosheath, the power spectral densities (PSDs) of magnetic fluctuations are first calculated with a continuous magnetic field data series, and then the values of spectral indices in the frequency between 1 and 16 Hz are determined by linear fitting. In the Martian magnetosheath, the median local proton gyrofrequency is lower than 0.6 Hz (Ruhunusiri et al., 2017). So, the frequency range of 1–16 Hz is always above the proton gyrofrequency, which indicates that it is a kinetic frequency range.

Observation Results

Among the 137 small-scale MH events, we first show an example observed in the Martian magnetosheath by MAVEN on 05 February 2016. **Figure 1**(A1-A2) shows the measured magnitude and three components of the magnetic field vector. The observed MH is located at 16:37:48.600 UT, which has an obvious dip in magnetic field magnitude. The two boundaries of this MH, which are determined by the nearest points with a

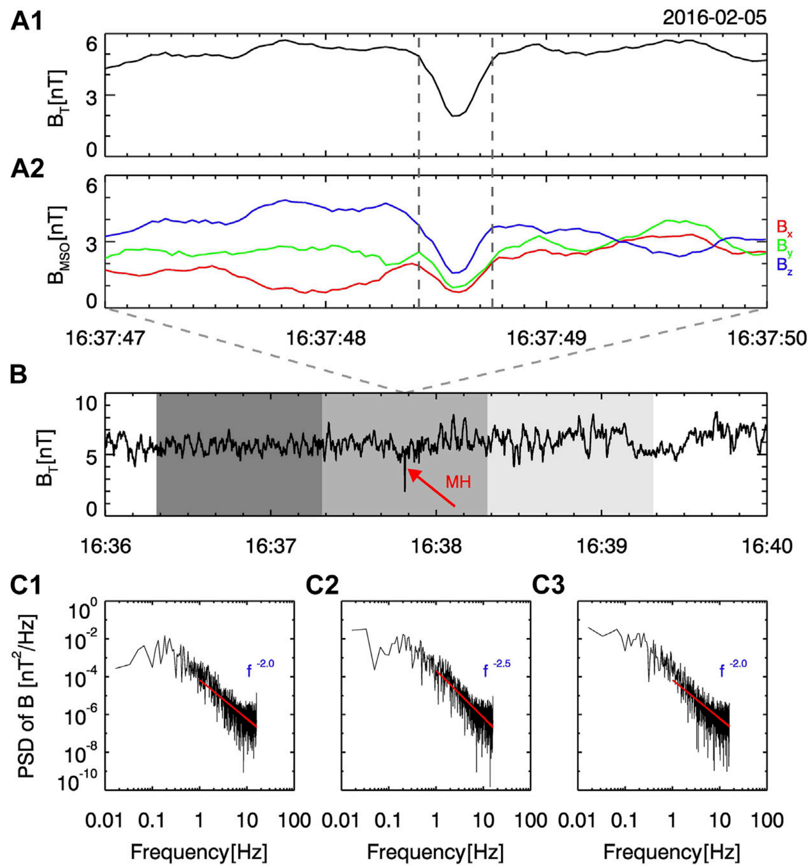

FIGURE 1 | Small-scale magnetic hole observed in the Martian magnetosheath by MAVEN on 05 February 2016. **(A1)** Magnetic field magnitude. **(A2)** Three components of the magnetic field (red, cyan, and blue are the x, y, and z components of the magnetic field, respectively) in MSO coordinates. The time interval of the small-scale magnetic hole is marked by two vertical gray dashed lines in **(A1)** and **(A2)**. **(B)** Time series of the total magnetic field. The dark gray region is the 1-min window before the MH, the gray region is the 1-minute window containing the MH, and the light gray region is the 1-min window after the MH. **(C1-C3)** PSDs computed by the 1-min window before, containing, and after the MH, respectively.

magnetic field magnitude greater than B – δ, are marked by two vertical gray dashed lines. The time interval of this MH is 0.34 s. The rotation angle $\Delta\varphi$ of this event is 4°. The background solar wind speed is 277 km/s, the duration of this MH is t = 0.34 s, and the proton thermal gyroradius ρ_i is 188 km. Based on these parameters, along the direction of the solar wind flow, this MH has a scale of 102 km which is about 0.54 ρ_i. So, this event is a small-scale MH event. In this small-scale MH event, the magnetic field magnitude depression B_{min}/B is 0.39. **Figure 1B** shows the magnetic field magnitude in a 4-min window. Three 1-min windows, which, respectively, are before, contain, and are after this small-scale MH, are marked by three different depths of gray shaded areas in **Figure 1B**. In each 1-min window, the fast Fourier transform is performed on 32-Hz magnetic field data, and then the PSDs of magnetic fluctuations are obtained. We have also calculated the spectral indices in the kinetic range of 1–16 Hz by using a linear fitting method. The results are shown in **Figure 1**(C1-C3). We denote α_c as the spectral index value α_c of the 1-min window containing the MH. α_b and α_a are denoted as the spectral index value α_b of the 1-min window before and after the one containing the MH, respectively. In this event, α_c is 2.5, and α_b and α_a are both 2.0. The spectral index value of the magnetic fluctuations with a small-scale MH can increase by 0.5 than the value of the ambient plasma environment. It indicates that the small-scale MH can significantly influence the spectral indices of magnetic fluctuations.

The presence of small-scale MHs can influence the spectral index because they have high-frequency spectral components. We try to check whether this transient structure can influence turbulence cascade and play an important role in the dissipation of magnetic energy. The wavelet analysis of the magnetic field fluctuation is employed to confirm the effect of this MH. The results of the wavelet analysis are shown in **Figure 2A**. The color contour shows the wavelet spectrograph of the magnetic field data, and the red line is the time series of the magnetic field magnitude. It can be found that the magnetic field fluctuation with frequencies ranging from 1 to 4 Hz has an obvious enhancement inside this MH, while there is no such enhancement outside this transient structure. If we just exclude this magnetic structure, the spectral index has a value of 2.0 during the 1-min interval before the MH, and 2.1 during the 1-min interval after the MH, which are shown in

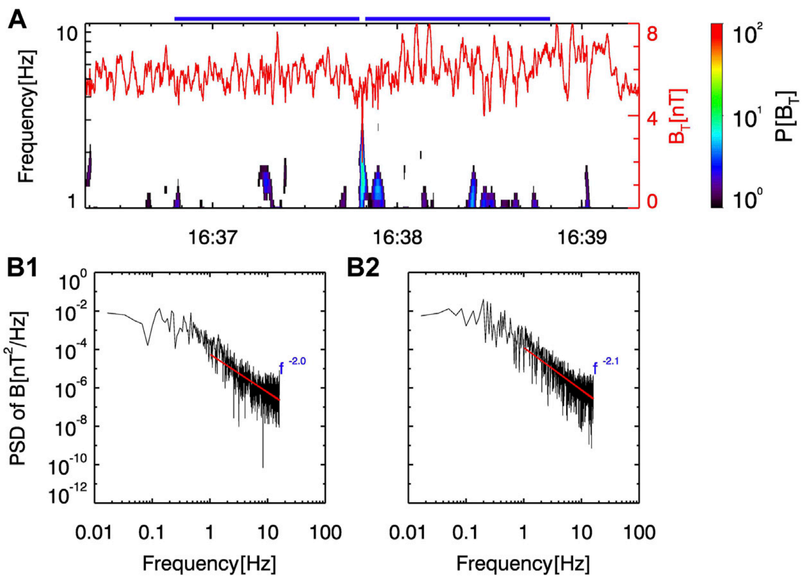

FIGURE 2 | (A) Wavelet spectrograph of the magnetic field data, and the red curve is the time series of the magnetic field magnitude; **(B1)** the PSDs computed by the 1-min window marked by the left blue bar in (A); **(B2)** the PSDs computed by the 1-min window marked by the right blue line in (A).

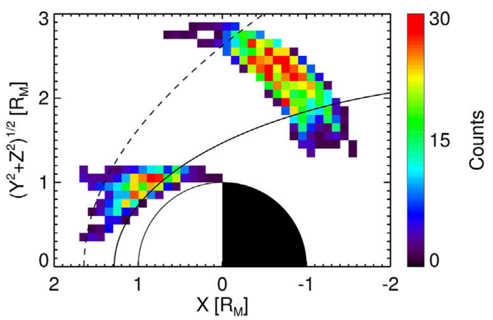

FIGURE 3 | Distribution of the orbit coverage shown in a cylindrical coordinate system. The bin size is 0.1 R_M. The black solid and dashed curves indicate the induced magnetopause boundary and bow shock adopted from Vignes et al. (2000), respectively.

Figure 2(B1) and (B2), respectively. These values are almost the same as those in **Figure 1**(C1) and (C3). Thus, the small-scale MHs seem to not affect the properties of the ambient magnetic fluctuation at least in this event, but the MHs can indeed influence the spectral index by their high-frequency spectral components.

To obtain the statistical features of spectral indices in the kinetic range 1–16 Hz of magnetic fluctuations in the Martian magnetosheath, a 3-min window used in our example event is employed in this study. The orbit coverage of the Martian magnetosheath during February 2016 is shown in **Figure 3**. Cells in a cylindrical coordinate system with a size $0.1 \times 0.1\, R_M$ are used. The black solid and dashed curves indicate the empirical locations of the induced magnetosphere boundary (IMB) and bow shock, respectively (Vignes et al., 2000). The color represents the counts of 3-min windows in each cell. There are more counts at the nightside than that at the dayside. It could be caused by slower speed near the apogee.

The spectral indices in the kinetic range 1–16 Hz for each event are calculated with this 3-min magnetic field data series. To determine whether small-scale MHs influence the spectral index value around the magnetosheath environment, we calculated power spectra at the 1–16 Hz frequency range in three 1-min windows like the example shown in **Figure 1**: a time interval containing the MH, a time interval before the one containing the MH, and a time interval after the one containing the MH. Then, the spectral index values α_b, α_c, and α_a in each 1-min window can be obtained by the linear fitting, respectively. Cells with a size $0.1 \times 0.1\, R_M$ and the median value of spectral indices in each cell are used to obtain the spectral index value distribution of all 137 small-scale MHs corresponding to these three different 1-min windows. **Figure 4** displays the distributions of the median values of (A) α_b, (B) α_c, and (C) α_a, respectively. The spectral indices of magnetic fluctuations of these three cases have different values in some cells.

Figures 4A,C give the magnetic fluctuations without small-scale MHs. The distributions of spectral indices at the dayside and the nightside of the Marian magnetosheath are different. At the nightside, the occurrence rate (number of events per hour) is mainly in the range from 2.3 to 2.6, while at the dayside, the occurrence rate mainly ranges from 1.7 to 3.2. Ruhunusiri et al. (2017) have found that the spectral index value can vary from 1.9 to 3.2 for the kinetic range in the Martian magnetosheath. Our results are consistent with theirs. In addition, as shown in **Figures 4A,C**, it can be found that the spectral index near bow shock is smaller than that near the IMB at the nightside. The value of spectral indices in the kinetic range gradually decreases from the region near the bow shock to the region near the IMB. Since there are not enough data at the dayside, this trend is not obvious. In

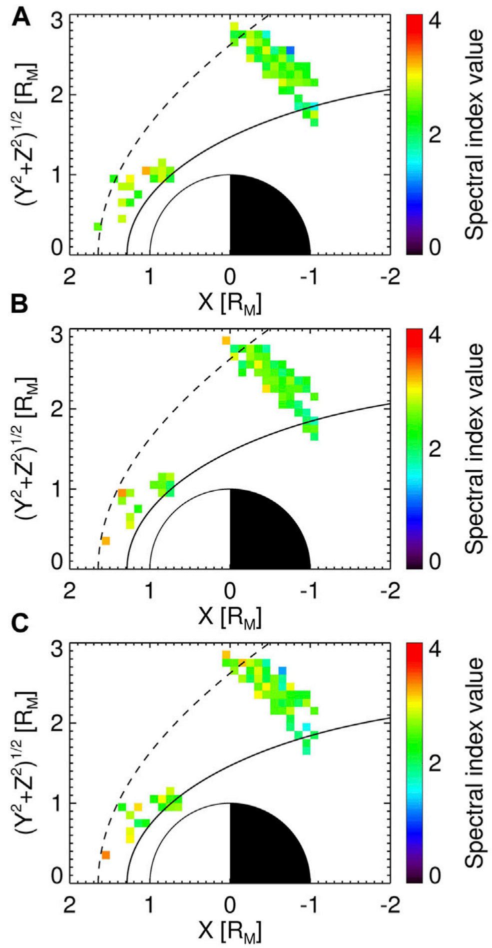

FIGURE 4 | Spectral index value distributions: **(A)** the median value of the spectral indices computed by 1-min data before each small-scale magnetic hole; **(B)** the median value of the spectral indices computed by 1-min date containing a small-scale magnetic hole; **(C)** the median value of the spectral indices computed by 1-min date after each small-scale magnetic hole.

kinetic range. **Table 1** has shown the minimum, maximum, median, and mean values and the standard deviation of α and Δα at the dayside and nightside.

DISCUSSIONS

The Martian magnetosheath is a turbulent plasma environment (Mazelle et al., 2004; Ruhunusiri et al., 2017). Ruhunusiri et al. (2017) have first investigated the global features of magnetic fluctuations in the Martian space environment and found that magnetic fluctuations in the Martian magnetosheath are dominated by some local structures and processes. In our study, we have studied magnetic fluctuations associated with small-scale MHs in the Martian magnetosheath and aimed to find the effect of these MHs on the spectral indices in the kinetic frequency range 1–16 Hz. The spectral index value is mainly from 2.3 to 2.6 at the nightside of the Martian magnetosheath. At the dayside of the Martian magnetosheath, the spectral indices are around 2.8 and 1.8 for most events. Ruhunusiri et al. (2017) have found that for the kinetic range, the spectral indices of sheath fluctuations are around 2.9 in the central part of the Martian magnetosheath, while the indices have a flatter distribution from 2.0 to 2.9 near the induced magnetosphere boundary. In our study, the value of the spectral index is in a similar range.

In our study, the value of spectral indices has a decreasing tendency from the region near the bow shock to the region near the IMB at the nightside. However, the spectral index values at the dayside have no obvious trend. In Ruhunusiri et al. (2017), the plasma processes near the IMB have an obvious effect on the value of spectral indices. It can be found that the size of the magnetosheath at the dayside is very great. So, magnetic fluctuations at the dayside can be more strongly affected by the plasma processes than those at the IMB. It may lead to the difference in the index value at the dayside and nightside. Additionally, the interplanetary magnetic field mainly is along *Y* direction near the orbit of Mars. So, the data points at the dayside are mainly downstream of the quasi-perpendicular bow

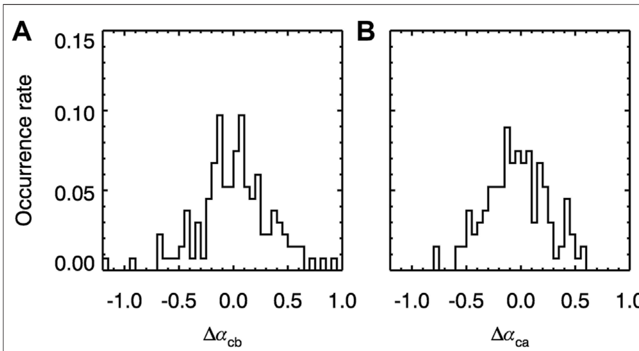

FIGURE 5 | (A) Histograms of the difference of the spectral index value between the time interval containing the MH and the time interval before the one containing the MH; **(B)** histograms of the difference of the spectral index value between the time interval containing the MH and the time interval after the one containing the MH.

the future, we would like to use more events to analyze the features at the dayside.

For each MH event, we have computed $\Delta\alpha_{cb} = \alpha_c - \alpha_b$ and $\Delta\alpha_{ca} = \alpha_c - \alpha_a$, and then use the distributions of $\Delta\alpha_{cb}$ and $\Delta\alpha_{ca}$ to estimate the effect of small-scale MHs on the spectral index value of magnetic fluctuations in the kinetic range. The histograms of (A) $\Delta\alpha_{cb}$ and (B) $\Delta\alpha_{ca}$ are shown in **Figure 5**. It can be found that distributions of $\Delta\alpha_{cb}$ and $\Delta\alpha_{ca}$ have similar features. There are events with negative $\Delta\alpha$ more than that with positive $\Delta\alpha$. For most of the events, both $\Delta\alpha_{cb}$ and $\Delta\alpha_{ca}$ are mainly in the region with $-0.3 < \Delta\alpha < 0.3$. It indicates that small-scale MHs mainly lead to a variation of the spectral index value, but such a variation is not very significant. However, there are also 44 events (32% of total events) with the absolute value of $\Delta\alpha_{cb}$ larger than 0.3, and 38 events (27% of total events) with the absolute value of $\Delta\alpha_{ca}$ larger than 0.3. In these events, the spectral index is not a credible indicator for the estimation of magnetic energy dissipation in the

TABLE 1 | Minimum, maximum, median, and mean values and the standard deviation of α and Δα at the dayside and the nightside.

	α and Δα	Minimum	Maximum	Median value	Mean value	Standard deviation
Dayside	α_c	1.84	3.29	2.55	2.60	0.37
	$\Delta\alpha_{cb}$	−1.12	0.97	0.00	−0.07	0.46
	$\Delta\alpha_{ca}$	−0.72	1.01	0.00	0.00	0.37
Nightside	α_c	1.60	3.31	2.38	2.35	0.37
	$\Delta\alpha_{cb}$	−0.62	0.89	0.10	0.09	0.29
	$\Delta\alpha_{ca}$	−0.74	0.60	0.03	0.02	0.28

shock, while the data points at the nightside are downstream of the quasi-parallel bow shock in our study. Xiao et al. (2021) found that the geometry of the Venusian bow shock influences the spectral index value of magnetic fluctuations. Like Venus, the difference in the spectral index value of magnetic fluctuations at the dayside and nightside could be partly due to the geometry of the Martian bow shock.

Small-scale MHs are typical sub-proton-scale magnetic structures that are always detected in the turbulent Martian, terrestrial, and Venusian magnetosheaths (e.g., Huang et al., 2017a; Yao et al., 2017; Goodrich et al., 2021; Wu et al., 2021). The PIC simulation results have shown that small-scale MHs can arise during the turbulent evolution of the plasma (Haynes et al., 2015; Roytershteyn et al., 2015). Whether small-scale MHs can contribute to the properties of magnetic fluctuations is still an open question. Based on the statistical analysis of 137 small-scale MHs, we have calculated the spectral indices of magnetic fluctuations in the kinetic range (1–16 Hz) for three time intervals associated with an identified MH: a time interval containing the MH, a time interval before the one containing the MH, and a time interval after the one containing the MH. Our results have shown that small-scale MHs have high-frequency spectral components and thus can influence the spectral index in the high-frequency range. For most events, the small-scale MHs lead to a variation in the spectral index. In more than 20% of the events, such a variation can exceed 0.3.

Small-scale MHs could affect the spectral index value in the kinetic range by the following mechanism. The small-scale MH is an isolated magnetic dip always with a duration from 0.1 to 1 s (Wu et al., 2021). It can lead an extra power enhancement around several hertz. When we calculated the spectral index in the range [1, 16] Hz, the extra power enhancement can lead to the change of the spectral index value. For example, as shown in **Figure 1**(C2), the MH is an isolated peak with a duration of 0.34 s, which can lead to an extra power enhancement around 3 Hz. The enhancement of power spectral density at the low-frequency part and the unchanged power spectral density at the high-frequency part would lead to an increase in the spectral index value. As a quasi-stable structure, the small-scale MH only enhances the power spectral density at a specific frequency, instead of changing the broadband spectrum. So during the calculation of the spectral index in the kinetic range, these MHs seem to cause some calculation errors. Therefore, during the analysis of the cascade of magnetic turbulence, using the spectral index alone as a diagnostic may not be convincing, especially in the presence of some transient structures.

Until now, it is unclear how small-scale MHs affect their plasma environment. Recently, Franco et al. (2019) have estimated correlation lengths of ultralow-frequency (ULF) waves around Mars and pointed out that wave fluctuations at the Martian magnetosheath may be correlated with the upper ionosphere. Their work renders a new way to understand the microphysical processes that occur within the Martian environment. We will work on the topic of the importance of small-scale MHs to Martian microphysics in the future.

SUMMARY AND CONCLUSION

In this study, we have analyzed magnetic fluctuations in the Martian magnetosheath using the MAVEN magnetic field data in February 2016. We have calculated the spectral indices in kinetic regimes for the 1-min window before and after the small-scale MHs and the 1-min window containing the small-scale MH. By the comparisons of the three intervals, we try to investigate whether small-scale MHs can influence the features of magnetic fluctuations and turbulence in the Martian magnetosheath. The main results are as follows:

1) The small-scale MHs can influence the spectral indices in the kinetic range of magnetic fluctuations by their high-frequency spectral components.
2) The small-scale MH lead to a variation in the spectral index in the kinetic range for most events.
3) For more than 20% of events, the value of the spectral index in the kinetic range can change by 0.3 due to the effect of small-scale MHs.

Our results have already confirmed that small-scale MHs can lead to a change in the spectral index in this kinetic range by the enhancement of the power spectral density at the frequency range [1, 16] Hz. Therefore, using the spectral index alone as a diagnostic sometimes is not enough convincing during the analysis of turbulence in planetary environments.

DATA AVAILABILITY STATEMENT

Publicly available datasets were analyzed in this study. These data can be found here: https://pds-ppi.igpp.ucla.edu/mission/MAVEN.

AUTHOR CONTRIBUTIONS

YC analyzed the MAVEN data and drew all the figures. MW conceptualized the study and produced the published results based on MAVEN physical data products. This study was on the leading of TZ. AD, MW, and TZ contributed substantially to the scientific interpretation of the results. All authors discussed the results and conclusions of the manuscript.

FUNDING

The work in China was supported by NSFC (grants 41774171, 41974205, 41774167, 41804157, and 41904156), and the pre-research project on Civil Aerospace Technologies (No. D020103) was funded by CNSA. The authors also acknowledge the Macau Foundation. MW was supported by a grant from the Key Laboratory of Geospace Environment, CAS. TZ was supported by the CAS Center for Excellence in Comparative Planetology. The MAVEN data are publicly available through the Planetary Plasma Interactions Node of the Planetary Data System (https://pds-ppi.igpp.ucla.edu/mission/MAVEN).

ACKNOWLEDGMENTS

We thank the entire MAVEN team and instrument leaders for high-quality data and convenient access.

REFERENCES

Acuña, M. H., Connerney, J. E. P., Wasilewski, P., Lin, R. P., Anderson, K. A., Carlson, C. W., et al. (1998). Magnetic Field and Plasma Observations at Mars: Initial Results of the Mars Global Surveyor mission. *Science* 279 (5357), 1676–1680. doi:10.1126/science.279.5357.1676

Alexandrova, O., Carbone, V., Veltri, P., and Sorriso-Valvo, L. (2008). Small-Scale Energy Cascade of the Solar Wind Turbulence. *ApJ* 674 (2), 1153–1157. doi:10.1086/524056

Alexandrova, O. (2008). Solar Wind vs Magnetosheath Turbulence and Alfvén Vortices. *Nonlin. Process. Geophys.* 15, 95–108. doi:10.5194/npg-15-95-2008

Balikhin, M. A., Sibeck, D. G., Runov, A., and Walker, S. N. (2012). Magnetic Holes in the Vicinity of Dipolarization Fronts: Mirror or Tearing Structures? *J. Geophys. Res.* 117 (8), 1–14. doi:10.1029/2012JA017552

Bertucci, C., Mazelle, C., Crider, D. H., Mitchell, D. L., Sauer, K., Acuña, M. H., et al. (2004). MGS MAG/ER Observations at the Magnetic Pileup Boundary of Mars: Draping Enhancement and Low Frequency Waves. *Adv. Space Res.* 33 (11), 1938–1944. doi:10.1016/j.asr.2003.04.054

Bowen, T. A., Bale, S. D., Bandyopadhyay, R., Bonnell, J. W., Case, A., Chasapis, A., et al. (2021). Kinetic-Scale Turbulence in the Venusian Magnetosheath. *Geophys. Res. Lett.* 48, e2020GL090783. doi:10.1029/2020GL090783

Bruno, R., and Carbone, V. (2013). The Solar Wind as a Turbulence Laboratory. *Living Rev. Solar Phys.* 10, 2. doi:10.12942/lrsp-2013-2

Chen, C. H. K., Klein, K. G., and Howes, G. G. (2019). Evidence for Electron Landau Damping in Space Plasma Turbulence. *Nat. Commun.* 10, 1–8. doi:10.1038/s41467-019-08435-3

Connerney, J. E. P., Espley, J., Lawton, P., Murphy, S., Odom, J., Oliversen, R., et al. (2015). The MAVEN Magnetic Field Investigation. *Space Sci. Rev.* 195 (1–4), 257–291. doi:10.1007/s11214-015-0169-4

Franco, A. M. S., Fränz, M., Echer, E., and Bolzan, M. J. A. (2019). Correlation Length Around Mars: A Statistical Study with MEX and MAVEN Observations. *Earth Planet. Phys.* 3 (6), 560–569. doi:10.26464/epp20190510.26464/epp2019051

Ge, Y. S., McFadden, J. P., Raeder, J., Angelopoulos, V., Larson, D., and Constantinescu, O. D. (2011). Case Studies of Mirror-Mode Structures Observed by THEMIS in the Near-Earth Tail during Substorms. *J. Geophys. Res.* 116 (1), 1–12. doi:10.1029/2010JA015546

Gershman, D. J., Dorelli, J. C., Viñas, A. F., Avanov, L. A., Gliese, U., Barrie, A. C., et al. (2016). Electron Dynamics in a Subproton-Gyroscale Magnetic Hole. *Geophys. Res. Lett.* 43 (9), 4112–4118. doi:10.1002/2016GL068545

Goldstein, M. L., Roberts, D. A., and Matthaeus, W. H. (1995). Magnetohydrodynamic Turbulence in the Solar Wind. *Annu. Rev. Astron. Astrophys.* 33, 283–325. doi:10.1146/annurev.aa.33.090195.001435

Goodrich, K. A., Bonnell, J. W., Curry, S., Livi, R., Whittlesey, P., Mozer, F., et al. (2021). Evidence of Subproton-Scale Magnetic Holes in the Venusian Magnetosheath. *Geophys. Res. Lett.* 48 (5), 1–9. doi:10.1029/2020GL090329

Haynes, C. T., Burgess, D., Camporeale, E., and Sundberg, T. (2015). Electron Vortex Magnetic Holes: A Nonlinear Coherent Plasma Structure. *Phys. Plasmas* 22 (1), 012309. doi:10.1063/1.4906356

Hollweg, J. V., and Markovskii, S. A. (2002). Cyclotron Resonances of Ions with Obliquely Propagating Waves in Coronal Holes and the Fast Solar Wind. *J. Geophys. Res.* 107, 1–7. doi:10.1029/2001JA000205

Huang, S. Y., Du, J. W., Sahraoui, F., Yuan, Z. G., He, J. S., Zhao, J. S., et al. (2017a). A Statistical Study of Kinetic-Size Magnetic Holes in Turbulent Magnetosheath: MMS Observations. *J. Geophys. Res. Space Phys.* 122 (8), 8577–8588. doi:10.1002/2017JA024415

Huang, S. Y., Sahraoui, F., Yuan, Z. G., He, J. S., Zhao, J. S., Contel, O. L., et al. (2017b). Magnetospheric Multiscale Observations of Electron Vortex Magnetic Hole in the Turbulent Magnetosheath Plasma. *ApJ* 836 (2), L27. doi:10.3847/2041-8213/aa5f50

Jakosky, B. M., Lin, R. P., Grebowsky, J. M., Luhmann, J. G., Mitchell, D. F., Beutelschies, G., et al. (2015). The Mars Atmosphere and Volatile Evolution (MAVEN) Mission. *Space Sci. Rev.* 195, 3–48. doi:10.1007/s11214-015-0139-x

Kiyani, K. H., Chapman, S. C., Khotyaintsev, Y. V., Dunlop, M. W., and Sahraoui, F. (2009). Global Scale-Invariant Dissipation in Collisionless Plasma Turbulence. *Phys. Rev. Lett.* 103 (7), 2007–2010. doi:10.1103/PhysRevLett.103.075006

Mazelle, C., Winterhalter, D., Sauer, K., Trotignon, J. G., Acuña, M. H., Baumgärtel, K., et al. (2004). Bow Shock and Upstream Phenomena at Mars. *Space Sci. Rev.* 111 (1–2), 115–181. doi:10.1007/978-0-306-48604-3_3

Roberts, O. W., Li, X., and Jeska, L. (2015). A Statistical Study of the Solar Wind Turbulence at Ion Kinetic Scales Using Thek-Filtering Technique and Cluster Data. *ApJ* 802, 2. doi:10.1088/0004-637X/802/1/2

Roytershteyn, V., Karimabadi, H., and Roberts, A. (2015). Generation of Magnetic Holes in Fully Kinetic Simulations of Collisionless Turbulence. *Phil. Trans. R. Soc. A.* 373, 20140151. doi:10.1098/rsta.2014.0151

Ruhunusiri, S., Halekas, J. S., Espley, J. R., Mazelle, C., Brain, D., Harada, Y., et al. (2017). Characterization of Turbulence in the Mars Plasma Environment with MAVEN Observations. *J. Geophys. Res. Space Phys.* 122 (1), 656–674. doi:10.1002/2016JA023456

Sahraoui, F., Belmont, G., Rezeau, L., Cornilleau-Wehrlin, N., Pinçon, J. L., and Balogh, A. (2006). Anisotropic Turbulent Spectra in the Terrestrial Magnetosheath as Seen by the Cluster Spacecraft. *Phys. Rev. Lett.* 96 (7), 075002. doi:10.1103/PhysRevLett.96.075002

Sun, W. J., Shi, Q. Q., Fu, S. Y., Pu, Z. Y., Dunlop, M. W., Walsh, A. P., et al. (2012). Cluster and TC-1 Observation of Magnetic Holes in the Plasma Sheet. *Ann. Geophys.* 30 (3), 583–595. doi:10.5194/angeo-30-583-2012

Sundberg, T., Burgess, D., and Haynes, C. T. (2015). Properties and Origin of Subproton-Scale Magnetic Holes in the Terrestrial Plasma Sheet. *J. Geophys. Res. Space Phys.* 120, 2600–2615. doi:10.1002/2014JA020856

Tsurutani, B. T., Lakhina, G. S., Verkhoglyadova, O. P., Echer, E., and Guarnieri, F. L. (2010). Magnetic Decreases (MDs) and Mirror Modes: Two Different Plasma β Changing Mechanisms. *Nonlin. Process. Geophys.* 17, 467–479. doi:10.5194/npg-17-467-2010

Tsurutani, B. T., Lakhina, G. S., Verkhoglyadova, O. P., Echer, E., Guarnieri, F. L., Narita, Y., et al. (2011). Magnetosheath and Heliosheath Mirror Mode Structures, Interplanetary Magnetic Decreases, and Linear Magnetic Decreases: Differences and Distinguishing Features. *J. Geophys. Res.* 116, A02103. doi:10.1029/2010JA015913

Uritsky, V. M., Slavin, J. A., Khazanov, G. V., Donovan, E. F., Boardsen, S. A., Anderson, B. J., et al. (2011). Kinetic-scale Magnetic Turbulence and Finite Larmor Radius Effects at Mercury. *J. Geophys. Res.* 116 (9), 1–14. doi:10.1029/2011JA016744

Vignes, D., Mazelle, C., Rme, H., Acuña, M. H., Connerney, J. E. P., Lin, R. P., et al. (2000). The Solar Wind Interaction with mars: Locations and Shapes of the bow Shock and the Magnetic Pile-Up Boundary from the Observations of the MAG/ER experiment Onboard Mars Global Surveyor. *Geophys. Res. Lett.* 27 (1), 49–52. doi:10.1029/1999GL010703

Vörös, Z., Baumjohann, W., Nakamura, R., Volwerk, M., Runov, A., Zhang, T. L., et al. (2004). Magnetic Turbulence in the Plasma Sheet. *J. Geophys. Res. Space Phy.* 109 (A11), 1–16. doi:10.1029/2004JA010404

Vörös, Z., Yordanova, E., Khotyaintsev, Y. V., Varsani, A., and Narita, Y. (2019). Energy Conversion at Kinetic Scales in the Turbulent Magnetosheath. *Front. Astron. Space Sci.* 6, 60. doi:10.3389/fspas.2019

Vörös, Z., Zhang, T. L., Leubner, M. P., Volwerk, M., Delva, M., Baumjohann, W., et al. (2008). Magnetic Fluctuations and Turbulence in the Venus Magnetosheath and Wake. *Geophys. Res. Lett.* 35 (11), 1–5. doi:10.1029/2008GL033879

Wang, G. Q., Volwerk, M., Xiao, S. D., Wu, M. Y., Hao, Y. F., Liu, L. J., et al. (2020a). Three-dimensional Geometry of the Electron-Scale Magnetic Hole in the Solar Wind. *ApJL* 904 (1), L11. doi:10.3847/2041-8213/abc553

Wang, G. Q., Zhang, T. L., Xiao, S. D., Wu, M. Y., Wang, G., Liu, L. J., et al. (2020b). Statistical Properties of Sub-Ion Magnetic Holes in the Solar Wind at 1 AU. *J. Geophys. Res. Space Phys.* 125 (10), A028320. doi:10.1029/2020JA028320

Wu, M., Chen, Y., Du, A., Wang, G., Xiao, S., Peng, E., et al. (2021). Statistical Properties of Small-Scale Linear Magnetic Holes in the Martian Magnetosheath. *ApJ* 916 (2), 104. doi:10.3847/1538-4357/ac090b

Xiao, S. D., Wu, M. Y., Wang, G. Q., Chen, Y. Q., and Zhang, T. L. (2021). The Spectral Scalings of Magnetic Fluctuations Upstream and Downstream of the Venusian bow Shock. *Earth Planets Space* 73 (1), 13. doi:10.1186/s40623-020-01343-7

Xiao, S. D., Zhang, T. L., and Vörös, Z. (2018). Magnetic Fluctuations and Turbulence in the Venusian Magnetosheath Downstream of Different Types of bow Shock. *J. Geophys. Res. Space Phys.* 123 (10), 8219–8226. doi:10.1029/2018JA025250

Yao, S. T., Hamrin, M., Shi, Q. Q., Yao, Z. H., Degeling, A. W., Zong, Q. G., et al. (2020). Propagating and Dynamic Properties of Magnetic Dips in the Dayside Magnetosheath: MMS Observations. *J. Geophys. Res. Space Phys.* 125 (6), 1–16. doi:10.1029/2019JA026736

Yao, S. T., Wang, X. G., Shi, Q. Q., Pitkänen, T., Hamrin, M., Yao, Z. H., et al. (2017). Observations of Kinetic-size Magnetic Holes in the Magnetosheath. *J. Geophys. Res. Space Phys.* 122 (2), 1990–2000. doi:10.1002/2016JA023858

Zhang, T. L., Baumjohann, W., Russell, C. T., Jian, L. K., Wang, C., Cao, J. B., et al. (2009). Mirror Mode Structures in the Solar Wind at 0.72 AU. *J. Geophys. Res.* 114 (10), 1–5. doi:10.1029/2009JA014103

Zhang, T. L., Russell, C. T., Baumjohann, W., Jian, L. K., Balikhin, M. A., Cao, J. B., et al. (2008). Characteristic Size and Shape of the Mirror Mode Structures in the Solar Wind at 0.72 AU. *Geophys. Res. Lett.* 35 (10), 2–5. doi:10.1029/2008GL033793

Zhang, T. L., Schwingenschuh, K., Lichtenegger, H., Riedler, W., Russell, C. T., and Luhmann, J. G. (1991). Interplanetary Magnetic Field Control of the Mars bow Shock: Evidence for Venuslike Interaction. *J. Geophys. Res.* 96 (A7), 11265–11269. doi:10.1029/91JA01099

Zimbardo, G., Greco, A., Sorriso-Valvo, L., Perri, S., Vörös, Z., Aburjania, G., et al. (2010). Magnetic Turbulence in the Geospace Environment. *Space Sci. Rev.* 156 (1–4), 89–134. doi:10.1007/s11214-010-9692-5

Conflict of Interest: The authors declare that the research was conducted in the absence of any commercial or financial relationships that could be construed as a potential conflict of interest.

Publisher's Note: All claims expressed in this article are solely those of the authors and do not necessarily represent those of their affiliated organizations, or those of the publisher, the editors, and the reviewers. Any product that may be evaluated in this article, or claim that may be made by its manufacturer, is not guaranteed or endorsed by the publisher.